Robotics and Autonomous Systems 59 (2011) 142–150

Contents lists available at ScienceDirect

Robotics and Autonomous Systems

journal homepage: www.elsevier.com/locate/robot

Efficient force distribution and leg posture for a bio-inspired spider robot

R. Vidoni *, A. Gasparetto

DIEGM, Department of Electrical, Management and Mechanical Engineering, University of Udine, Via delle Scienze, 208, 33100 Udine, Italy

ARTICLE INFO

Article history:
Received 19 October 2009
Received in revised form
13 October 2010
Accepted 20 October 2010
Available online 25 November 2010

Keywords:
Climbing spider robot
Legged mechanism
Bio-mimesis
Force distribution
Adhesion

ABSTRACT

Legged walking and climbing robots have recently achieved important results and developments, but they still need further improvement and study. As demonstrated by recent works, bio-mimesis can lead to important technical solutions in order to achieve efficient systems able to climb, walk, fly or swim (Saunders et al., 2006 [36], Ayers, 2001 [25], Safak and Adams, 2002 [26]). In this paper, taking into account the anatomy and the adhesive and locomotion capabilities of the spider (i.e., an eight-legged system), we present on the one hand a study of the foot force and torque distribution in different operative and slope conditions and, on the other hand, a posture evaluation by comparing different leg configurations in order to minimize the torque effort requirements.

1. Introduction

Most of the vehicles that we are familiar with use wheels for their locomotion. They can achieve high speed and relatively small control complexity but, even with complex suspension systems, they present a lot of limitations in irregular and rough terrains (e.g., hazardous environments and uneven ground). With legged systems, most of the difficulties can be overcome thanks to the flexibility and ground adaptation. Indeed, the opportunity to choose between different available solutions and to adapt and control the position of the center of mass of the system allows avoiding slippage and overturns due to terrain irregularities. The costs that have to be paid are lower speed of locomotion and higher complexity of the control with respect to wheeled systems. However, bio-inspired locomotion controllers based on central pattern generators (CPGs; see [1]), i.e., neural circuits capable of producing coordinated patterns of high-dimensional rhythmic output signals while receiving only simple input signals, and on reflexive controllers, i.e., Cruse control for the coordination of the legs [2,3], are looking to fill the gap.

Moreover, due to the fact that the legs are independently controlled, legged systems have a large number of degrees of freedom (DOFs) to be coordinated in order to control the position, balance the forces (e.g., load, external forces) and consume as little energy as possible. Since the task of finding an optimal force allocation should be done in real time, fast algorithms and control functions have to be used, as also when a body force command solution is not achievable and a new plan has to be formulated.

Legged robots have a body and a number of articulated legs that start from it. Each of these kinematic chains can be viewed as a manipulator that acts like a limb and contributes to the overall position and equilibrium of the structure.

In order to evaluate and create an effective legged robot, the idea is to draw inspiration from nature. In nature, different legged systems able to walk and climb different surfaces with a low energetic consumption and high autonomy can be found. Indeed, safe attachment to and easy detachment from smooth substrates is a major feature of a diverse range of animal species. Attachment without using fluids, so-called dry adhesion, is exploited by geckos and *Evarcha arcuata* spiders by means of fibrillar elements [4–7].

The adhesion force seems to be related to the approaching angle between the attaching elements and the surface: the maximum adhesion condition is reached when the angle is around 30°; a sliding condition occurs when the angle is smaller, and detachment occurs when the angle is bigger [8,9].

In this work our attention is focused on a bio-mimetic spider robot.

Starting from the kinematic model and simulator (Fig. 1), which are the result of a previous biological and kinematic study [10,11], the static and quasi-static problems applied to the spider eight-legged system in different slope conditions are solved.

In Section 2, the analysis of the different theories and approaches related to the force and torque foot distribution that can be found in literature [12–24] are reviewed.

In Section 3, the theory of the optimal force distribution is presented and extended in order to search for an effective result

* Corresponding author. Tel.: +39 0432 558257x8041; fax: +39 0432 558251.
E-mail addresses: renato.vidoni@uniud.it, renato.vidoni@mechatronics.it (R. Vidoni), gasparetto@uniud.it (A. Gasparetto).

0921-8890/$ – see front matter © 2010 Elsevier B.V. All rights reserved.
doi:10.1016/j.robot.2010.10.001

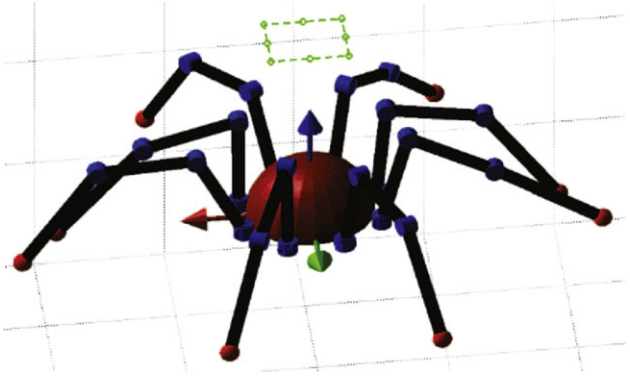

Fig. 1. Kinematic model of the spider robot. Each leg is composed of three links and three joints (one universal and two revolute pairs; see [10,11]).

for the spider system in all working conditions (i.e., flat, vertical and inverted surfaces).

In Section 4 an analysis of the overall amount of torque that has to be applied for maintaining different configurations and a comparison between different bio-mimetic postures and conditions for the legs is made.

Finally, concluding remarks and future work directions are presented in Section 5.

2. Legged robots: the force distribution problem (FDP)

The complexity of light legged robots, such as six-legged and four-legged robots, is due to the different kinematic chains (i.e., legs) that during the locomotion have to develop two different actions: those that are in a rested condition have to support and shift the body while balancing the forces; the legs in flight have to reach the future support position.

Moreover, due to the existence of four actuated joints in each leg, as in [10,11], the octopod model has a redundant actuation leading to more active joints than the number of robot degrees of freedom. Therefore, there are fewer force moment balance equations than unknown design variables, and the mathematical solution of these equations is not unique, due to the presence of a non-squared matrix. Looking at the real world, there are some physical constraints that have to be taken into account (i.e., the contact nature, friction, adhesion, torque limits) and that can be represented only through inequalities due to the nature of the contact.

An effective approach is the one based on the distribution of forces that try to solve the so-called *force distribution problem* (FDP; see, e.g., [13]). Each leg that touches and supports the body applies a certain force (f_d) on the support point that is balanced by means of an (equal and opposite) reaction force (f_r) of the substrate. f_d is the distributed force because it represents the distributed component of the external forces and moments applied on that leg. Hence, each leg can be considered as a manipulator anchored to the body that has to be able to generate on the tip of the last limb of the leg (i.e., the end-effector) an f_d force in order to create a static equilibrium. The geometry of the structure and the position of the legs produce the distribution of forces and moments on the legs. Since the mathematical solution is not unique and the physical constraints are only inequalities, the FDP involves the optimization of the force for the legs. Then, the FDP can be formulated as a nonlinear constrained programming problem under nonlinear equality and inequality constraints.

In the literature, several approaches and algorithms have been proposed for solving and finding the optimal solution of the FDP for legged robots. There are four main methods that can be studied and evaluated for a real implementation of the control.

1. Linear-programming (LP) method [14].
2. Compact-dual LP (CDLP) method [16].
3. Quadratic programming (QP) method [21].
4. Analytical method [22].

In comparison with the existing literature, several original features of this work can be remarked upon.

The spider is an eight-legged system, whereas usually six-legged and four-legged robots are studied. No applications of the FDP problem for an eight-legged system have been found in the literature. As a consequence, at least four legs are in contact with the substrate in the support phase condition (i.e., four legs in contact and four legs in flight) and the hypothesis adopted for six-legged robots in order to reduce the complexity of the system [22] cannot be applied.

Moreover, the spider robotic system must be able to walk and climb on different slope conditions up to the inverted condition; hence, the adhesive capabilities have to be taken into account.

Finally, in the model presented in this work, each spider leg has four DOFs while in the literature the number of DOFs of the eight-legged robots is usually three or less [25–27].

Thus, the present study is more general with respect to all the other studies dealing with legged systems. In particular, not only the friction force but also the adhesion forces have to be taken into account in order to simulate and control the system in the climbing phases.

The artificial attaching systems developed until now [28–31] do not reach the adhesive capabilities of the real ones, and usually degrade themselves with use; as a consequence, in order to evaluate and simulate an efficient model, the biological characteristics and adhesive capabilities of the spider *E. arcuata* [6,7] will be used to evaluate and solve the FDP.

Concerning the adhesion constraint, it has to be stressed that a leg can be considered in contact with the substrate only if the absolute value of the distributed forces on the chosen leg is less than the maximum adhesive force tolerable. The adhesion system is activated by the spider when an active grip is required, at least in all the cases in which the friction cone is violated. In Fig. 2, three limit conditions are depicted: in Fig. 2(a), contact with a flat floor, in Fig. 2(b), contact with a vertical wall, and in Fig. 2(c) the upside-down condition when the system is in adhesion on a ceiling.

3. Static analysis

3.1. Problem formulation

The system of forces acting on an octopod robot is depicted in Fig. 3, where both the body and the legs are represented in a generic way. According to the FDP formulation, only the external forces $\mathbf{F} = [F_x, F_y, F_z]^T \in \Re^3$, the external moments applied to the body $\mathbf{M} = [M_x, M_y, M_z]^T \in \Re^3$ and the position of the points of contact of the n supporting legs $\mathbf{P}_i = [x_i, y_i, z_i]$ are necessary. The global reference system B is placed at the center of mass of the body. By considering that the generalized forces applied on the body are totally supported by the legs, letting $\mathbf{f}_i = [f_{ix}, f_{iy}, f_{iz}]$ be the vector of the distributed forces on the leg i (moments on the feet are neglected), the force–moment static equilibrium equation system of the robot can be written as

$$\begin{cases} F_x = \sum_{i=1}^{n} f_{ix} \\ F_y = \sum_{i=1}^{n} f_{iy} \\ F_z = \sum_{i=1}^{n} f_{iz}. \end{cases} \tag{1}$$

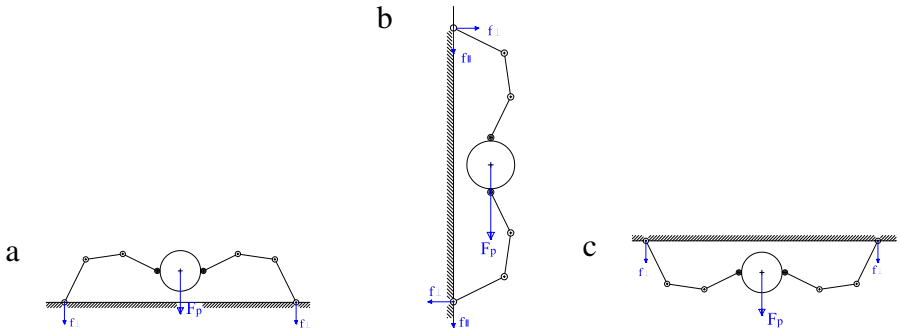

Fig. 2. Force distribution for two legs in different slope conditions. F_P is the weight of the system and $f_\perp$ and $f_\parallel$ the orthogonal and parallel components of the distributed force.

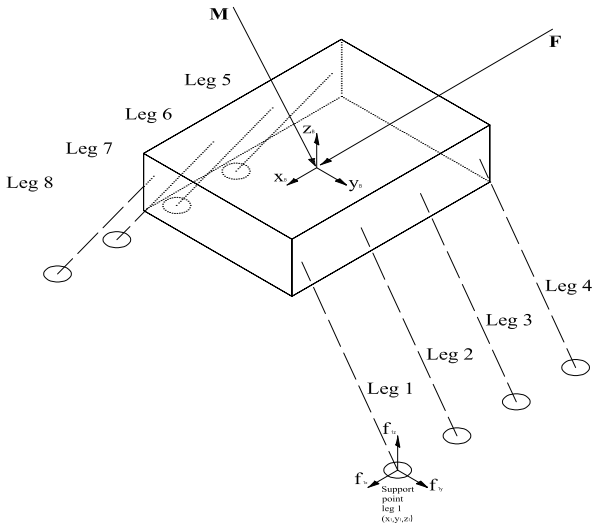

Fig. 3. Model of an eight-legged system for the FDP definition. Global reference system: $B = [x_B, y_B, z_B]$; leg contact points: $\mathbf{P}_i = [x_i, y_i, z_i]$; external forces: $\mathbf{F}$; external moments: $\mathbf{M}$; distributed forces on the legs: $\mathbf{f_i}$.

In matrix form, we obtain

$$\mathbf{F} = \mathbf{J_F}\mathbf{f} = \begin{bmatrix} 1 & 0 & 0 & \cdots & 1 & 0 & 0 \\ 0 & 1 & 0 & \cdots & 0 & 1 & 0 \\ 0 & 0 & 1 & \cdots & 0 & 0 & 1 \end{bmatrix} \begin{bmatrix} f_{1x} \\ f_{1y} \\ f_{1z} \\ \vdots \\ f_{nx} \\ f_{ny} \\ f_{nz} \end{bmatrix}. \tag{2}$$

By assuming that the substrate cannot exert an appreciable torque moment to the legs, the moments applied to the body have to be supported by the distributed forces:

$$\mathbf{M} = \sum_{i=1}^{n} [x_i, y_i, z_i]^T \times [f_{ix}, f_{iy}, f_{iz}]^T. \tag{3}$$

In matrix form, this can be written as

$$\mathbf{M} = \mathbf{J_M}\mathbf{f}$$

$$= \begin{bmatrix} 0 & -z_1 & y_1 & \cdots & 0 & -z_n & y_n \\ z_1 & 0 & -x_1 & \cdots & z_n & 0 & -x_n \\ -y_1 & x_1 & 0 & \cdots & -y_n & x_n & 0 \end{bmatrix} \begin{bmatrix} f_{1x} \\ f_{1y} \\ f_{1z} \\ \vdots \\ f_{nx} \\ f_{ny} \\ f_{nz} \end{bmatrix}. \tag{4}$$

By combining Eqs. (2) and (4), we obtain

$$\begin{bmatrix} \mathbf{F} \\ \mathbf{M} \end{bmatrix} = \mathbf{W} = \begin{bmatrix} \mathbf{J_F} \\ \mathbf{J_M} \end{bmatrix} \mathbf{f} = \mathbf{J_{FM}}\mathbf{f}. \tag{5}$$

The resulting system is under-definite, and infinite solutions for the distributed forces $\mathbf{f}$ can be found.

In order to find a solution ($\mathbf{f}$) to problem (Eq. (5)), the full row rank formula for the pseudoinverse can be used (the limit condition of all the feet in a line is not physically possible). Indeed, the Moore–Penrose generalized inverse solution is a good starting point because it belongs to the equilibrating force field, i.e., forces required to maintain equilibrium against an external load with no interaction components [20,32]. The rows of $\mathbf{J_{FM}} \in \Re^{6\times(3*n)}$ are all linearly independent; hence $\mathbf{J_{FM}}\mathbf{J_{FM}^T}$ is invertible, and the result can be expressed as

$$\mathbf{f} = \mathbf{J_{FM}^+}\mathbf{W} = \mathbf{J_{FM}^T}(\mathbf{J_{FM}}\mathbf{J_{FM}^T})^{-1}\mathbf{W}, \tag{6}$$

$\mathbf{J_{FM}^+}$ being the Moore–Penrose generalized inverse solution (also called the pseudoinverse).

The solution found gives a result that satisfies the equilibrium condition but, generally, does not match the physical limits and constraints. Indeed, the pseudoinverse solution ensures only the minimization of $\|\mathbf{J_{FM}}\mathbf{f} - \mathbf{W}\|$.

3.2. Problem solution optimization

The distributed forces at the feet of an octopod spider robot must comply with the physical constraints in order to be valid. All the supporting feet should not slip when the robot is in a rested condition or walking on the ground; hence the static friction constraint,

$$\sqrt{f_{ix}^2 + f_{iy}^2} \le \mu_c f_{iz}, \quad i = 1, \ldots, n, \tag{7}$$

where μ_c is the static friction coefficient of the substrate, has to be satisfied by the solution. The friction constraint can be geometrically represented as a cone with its axis orthogonal with respect to the support surface and with an "opening angle" equal to $\alpha = \arctan(\mu_c)$ (see Fig. 4).

In order to overcome the nonlinearities induced by the friction cone equations, it is possible to substitute the friction cone with an inscribed pyramid (see Fig. 4); hence we have a more restrictive constraint, expressed by

$$|f_{ix}| \le \mu_p f_{iz} \qquad |f_{iy}| \le \mu_p f_{iz}, \tag{8}$$

where $\mu_p = \mu_c/\sqrt{2}$.

A definite foot contact with the ground, in the case that the adhesive system is not exploited by the spider, exists only if there is an f_{iz} such that

$$f_{iz} \ge 0, \quad i = 1, \ldots, n. \tag{9}$$

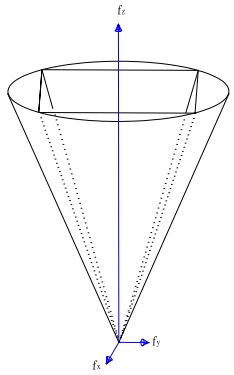

Fig. 4. The friction cone and pyramid: the "opening angle" is arctan μ_c.

Concerning the adhesion constraint, it can be satisfied if the absolute value of the sum of the distributed forces is less than the maximum allowable adhesion force, so that the spider does not fall down from an inclined or inverted surface.

Adhesion and friction are the two main constraints that must be taken into account while building the robot model. However, according to the different working conditions, either adhesion or friction has to be satisfied, thus leading to the three main cases.

CASE 1: when the spider system is on rest on a floor (see Fig. 2(a)), the weight of the system $\mathbf{F_p}$ works on the legs, creating forces $\mathbf{f}_\perp$ in the same direction of $\mathbf{F_p}$; in such a case, the limbs are loaded against the substrate and, hence, only the friction constraint is necessary.

CASE 2: if the robot is upside down on a ceiling, the force $\mathbf{F_p}$ acts on the legs in the direction opposite with respect to the contact plane, the $\mathbf{f}_\perp$ do not support the contact (see Fig. 2(c)) and, for a correct solution, the adhesion constraint has to be satisfied.

CASE 3: if a vertical surface is considered (see Fig. 2(b)), there are both legs with an orthogonal component of the distributed force directed towards the contact plane (friction constraint) and legs with an orthogonal component of the distributed force directed out of the contact plane (adhesion constraint).

By taking as the reference spider the *E. arcuata* [10,11] a realistic safety factor for the spider's adhesion is 160 [6,7], while the static friction coefficient μ is in the order of 0.1. Hence, if only the weight is considered, can act an adhesion or friction force on every leg: for adhesion, the maximum ratio between the adhesive force and f_{iz} is about 20; for friction, the ratio between the z-component and the other components becomes equal to μ, so two orders of magnitude less. The overall rule applied in the model can be summarized as follows. If the orthogonal component of the distributed forces is directed towards the support plane, the friction constraint has to be applied. In the other case, the adhesion constraint has to be imposed.

In order to apply the physical constraints, a preliminary solution for the components of the distributed forces has to be found. The chosen solution, which satisfies the equilibrium conditions, is the one obtained with the use of the pseudoinverse (Eqs. (5) and (6)).

However, one must check whether such a solution satisfies the physical (i.e., adhesion or friction) constraints; if not, a linear programming technique is considered in order to find a suitable solution. The friction constraint is the most restrictive, and it is governed by Eq. (8).

The object function to minimize has been chosen as

$$\min(A), A = \sum_i f_{iz} \quad i \in [\text{legs under friction constraint}]. \tag{10}$$

The linear programming technique has to take into account the friction constraints (Eq. (8)), the adhesion constraint and the static equilibrium equations (Eq. (6)). The overall system formulation becomes

$$\begin{aligned} &\text{find } \min(A) \text{ subject to} \\ &|f_{ix}| \le \mu_p f_{iz} \qquad |f_{iy}| \le \mu_p f_{iz} \\ &|f_j| < F_{\text{adesione}} \\ &\mathbf{f} = \mathbf{J}^+_{\mathbf{FM}}\mathbf{W} \\ &f_{iz} \le 0 \quad i \in \text{friction} \\ &f_{jz} > 0 \quad j \in \text{adhesion}. \end{aligned} \tag{11}$$

Table 1
Spider model main data.

Link	Biological name	Length
Body	Chephalothorax	Radius = 0.3 ∗ Meta-tarsus length
Link 1	Femur	0.8 ∗ Meta-tarsus length
Link 2	Tibia	0.75 ∗ Meta-tarsus length
Link 3	Meta-tarsus	1

3.3. Static problem solution

By exploiting the FDP results, it is possible to solve the static problem for each leg and compute the torques that must be applied to every active joint in order to reach and maintain a static equilibrium. The static equilibrium for a manipulator can be expressed as

$$\tau = \mathbf{J^T}(\mathbf{q})\gamma, \tag{12}$$

where $\tau \in \Re^{(n\times 1)}$ represents the vector of the torques applied to the joints (n actuated joints), $\gamma \in \Re^{(m\times 1)}$ the vector of forces and moments acting on the end-effector and $\mathbf{J}_i$ is the geometric Jacobian of the manipulator [33]. Hence, once the distributed forces are available, Eq. (12) can be used in order to find the torque required for each active joint of the legs (τ_i). For the i-th leg, it holds that

$$\tau_i = \mathbf{J}_i^T(\mathbf{q})\,\gamma_i, \tag{13}$$

where $\gamma_i = \left[f_{ix}, f_{iy}, f_{iz}, 0, 0, 0\right]^T$ and $\mathbf{J}_i$ is the geometric Jacobian of the considered leg. Taking into account the characteristics of the *E. arcuata* spider (see [6,7]): an estimated adhesion force per leg equal to 3×10^{-3} N, a mass of about 15×10^{-3} g, a static friction coefficient of 0.1 and the spider model dimensions in Table 1, the equilibrium condition and the optimal distribution forces can be checked for all the different conditions.

The rest condition is the basic configuration of the model, with all the legs in contact with the substrate and arranged in a radial manner with respect to the center of gravity of the body. This configuration has been chosen for the spider model as the initial and final configuration of the motion. In the rest configuration, the chosen values of the angles for the actuated joints of each leg are

$$\mathbf{q_i} = \begin{bmatrix} 0 \\ 1.551 \\ -2.117 \\ -0.005 \end{bmatrix}, \tag{14}$$

where the values are expressed in radians and $i = 1, \ldots, 8$.

The configuration and solution chosen between the available kinematic solutions is the one that reflects the C-shape configuration typical of spider systems (see Fig. 5(a)).

The theoretical and simulation results can be taken into account in the implementation of a real robotic system. Indeed, by exploiting the formulation and the analysis presented here, it is possible to calculate the requested torque values and, hence, a suitable type of actuation and size of the motors.

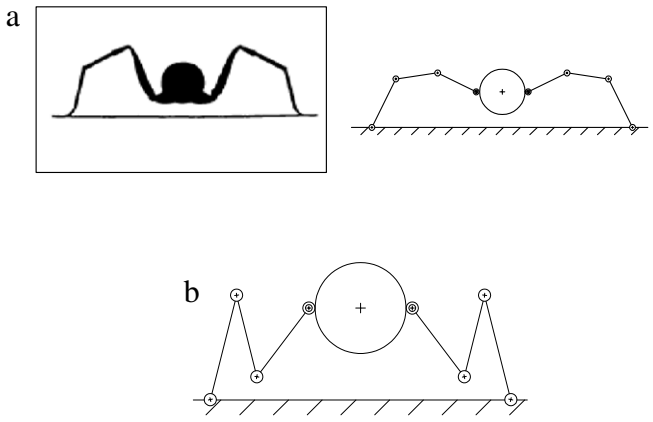

Fig. 5. C-shape and Z-shape models: (a) spider posture; (b) other arthropod or insect posture.

Table 2
Distributed forces and torques: rest configuration, floor case.

Leg	Distributed forces (μN)			Torques (μN m)			
	f_x	f_y	f_z	τ_1	τ_2	τ_3	τ_4
1	0	0	−18.394	0	−27.591	−27.295	−15.470
⋮	⋮	⋮	⋮	⋮	⋮	⋮	⋮
8	0	0	−18.394	0	−27.591	−27.295	−15.470

3.3.1. CASE 1

In this case, the spider model is considered on rest on a flat floor surface. By considering only the weight force and the configuration, the FDP solution found with the application of the Eq. (6) gives the results displayed in Table 2.

The results show how the distributed forces have a unique non-zero component, i.e., the vertical one, in the z direction.

The solution satisfies the physical friction constraints (Eq. (8)), and there is no need for optimization.

A Matlab® multibody simulator was implemented so as to assess the validity of the solution. The simulator is realized by exploiting the SimMechanics® toolbox, and a visual output is presented in Fig. 6. Each link is modeled by taking into account the geometric parameters and its mass and tensor of inertia. The joint position and torque values as well as the external forces and torques can be easily modified. Thus, the static problem solution can be directly put into the simulator and validated.

The required effort of the solution, considered as the sum of the absolute values of the torques at the joints, can be evaluated in comparison with the effort required for all the possible radial and C-shape configurations. The resulting minimum effort solution found, depicted in Fig. 7, is

$$\mathbf{q_1} = \cdots = \mathbf{q_8} = \begin{bmatrix} 0 \\ 1.052 \\ -2.618 \\ -0.002 \end{bmatrix}, \tag{15}$$

and the corresponding force and torque values are reported in Table 3.

The values of the requested torques are considerably lowered with respect to Table 2, and it can be reasonably said that there is a more efficient configuration and solution for the static problem for a flat floor surface with respect to the chosen C-shape one (Eq. (14)), namely the configuration shown in Fig. 7.

3.3.2. CASE 2

When the system is in adhesion on a ceiling and only the weight is considered, the adhesion constraints must be applied. This case can be treated as CASE 1 by switching the sign of the weight force. Hence, the result of the force distribution technique is the opposite of that in Table 2. Since the adhesion constraints are less restrictive with respect to the friction ones, the solution found does not need optimization.

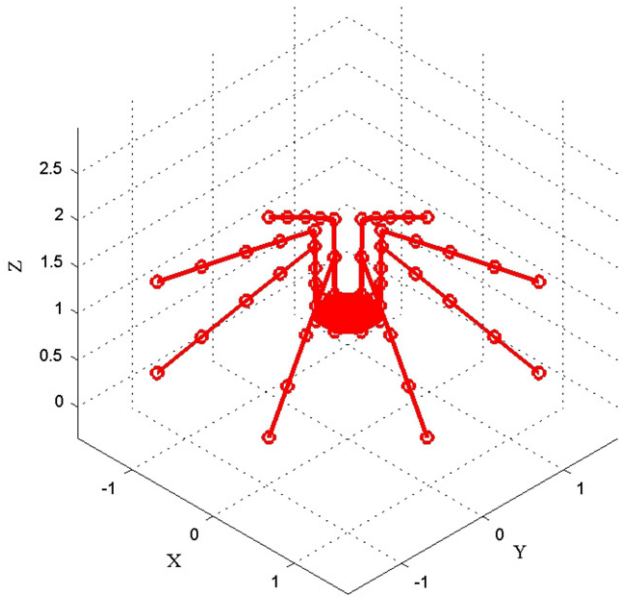

Fig. 6. Visual output of the Matlab® simulator.

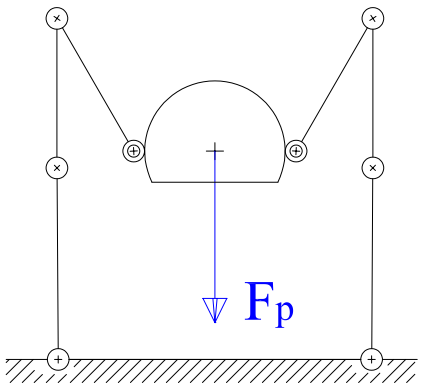

Fig. 7. Minimum effort configuration on a flat floor under the weight force.

Table 3
Minimum effort configuration on a flat floor: distributed forces and torques.

Leg	Distributed forces (μN)			Torques (μN m)			
	f_x	f_y	f_z	τ_1	τ_2	τ_3	τ_4
1	0	0	−18.394	0	−7.415	−0.119	−0.052
⋮	⋮	⋮	⋮	⋮	⋮	⋮	⋮
8	0	0	−18.394	0	−7.415	−0.119	−0.052

3.3.3. CASE 3

In the case of a vertical wall, there are both legs that are subjected to the adhesion constraint and legs under the friction constraint. When the system is on a vertical wall and the weight acts in the $-z$ direction, the force distribution solution can be found by considering the spider system at rest on the floor, and adding an external force, equal in value to the weight, directed orthogonally with respect to z, according to the orientation of the wall.

Table 4
Distributed forces for the rest configuration in a vertical wall case with both the pseudoinverse Eq. (6) (SX) and the linear programming technique with physical constraints (DX).

Leg	Distributed forces (μN)			Optimized forces (μN)		
	f_x	f_y	f_z	f_x	f_y	f_z
1	18.393	0	−2.832	0	0	0
2	18.393	0	−1.173	0	0	−9.457
3	18.393	0	1.173	36.787	0	9.452
4	18.393	0	2.832	36.787	0	0.004
5	18.393	0	2.832	36.787	0	0.004
6	18.393	0	1.173	36.787	0	6.556
7	18.393	0	−1.173	−0.001	0	−6.561
8	18.393	0	−2.832	0	0	0

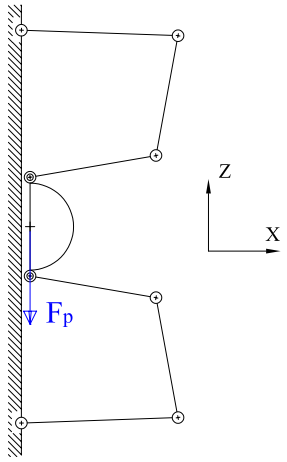

Fig. 8. Optimal configuration on a vertical wall.

First, the pseudoinverse technique is applied; then, the solution found is optimized in order to satisfy the friction constraints. The two sets of distributed forces, before and after optimization, are reported in Table 4.

The optimized solution shows two legs with distributed force components equal to zero along every axis. In order to satisfy the physical constraints, the optimization algorithm has distributed these forces on the other legs, augmenting the distributed forces where the adhesion is applied.

In order to evaluate the result from an energetic point of view, an iterative analysis has been applied to find the set of torques minimizing the overall effort requested to the robot (i.e., the sum of the absolute values of the torques at the joints). The radial C-shape configuration corresponding to the minimum effort state is given by

$$\mathbf{q_1} = \cdots = \mathbf{q_8} = \begin{bmatrix} 0 \\ 1.4 \\ -1.218 \\ -1.718 \end{bmatrix}. \tag{16}$$

Such a configuration is depicted in Fig. 8, and the torque values are reported in Table 6.

The optimized solution (Table 5) requires an overall effort of 349 μN m, while the minimum effort condition (Table 6) is 291 μN m. Looking at the minimum effort configuration, it is possible to show how the center of gravity of the spider system is very close to the surface; indeed, if the distance between the body and the surface increases, the moment applied by the distributed forces increases as well as the overall torque for the static equilibrium.

3.3.4. Other cases

Two significant situations are evaluated: the first is a typical configuration at the beginning of locomotion, and the second includes not only the weight but also some external forces and moments.

Table 5
Torques related to the optimized distributed forces for the rest configuration in a vertical wall.

Leg	Torques (μN m)			
	τ_1	τ_2	τ_3	τ_4
1	0	0	0	0
2	0	−14.186	−14.034	−7.954
3	−50.980	12.066	0.006	0.003
4	−21.116	−5.091	−32.275	−18.382
5	21.117	−5.091	−32.276	−18.382
6	50.981	7.722	−3.643	−2.102
7	0.001	−9.841	−9.736	−5.518
8	0	0	0	0

Table 6
Rest minimum effort configuration on a vertical wall.

Leg	Distributed forces (μN)			Torques (μN m)			
	f_x	f_y	f_z	τ_1	τ_2	τ_3	τ_4
1	0	0	0	0	0	0	0
2	0	0	−6.734	0	−6.196	−5.280	−0.234
3	36.787	0	6.732	−31.271	5.165	−6.848	−13.835
4	36.787	0	0	−12.952	−2.484	−29.279	−33.966
5	36.787	0	0	12.953	−2.484	−29.279	−33.966
6	36.788	0	4.791	31.271	3.379	−8.371	−13.902
7	0	0	−4.791	0	−4.408	−3.757	−0.167
8	0	0	0	0	0	0	0

Table 7
Optimum distributed forces and torques for the configuration adopted at the beginning of the step.

Leg	Distributed forces (μN)			Torques (μN m)			
	f_x	f_y	f_z	τ_1	τ_2	τ_3	τ_4
1	0	0	−33.741	0	−57.359	−50.591	−28.377
3	0	0	−38.797	0	−58.195	−56.784	−29.720
5	0	0	−39.695	0	−55.573	−55.175	−25.911
7	0	0	−34.917	0	−59.359	−51.554	−26.748

The starting step configuration has four legs in contact with the substrate: two of them are arranged in the direction of movement while the others are laterally disposed in order to support the system. The angular values of the pairs for the rested legs are

$$\mathbf{q_1} = \begin{bmatrix} 0 \\ 1.317 \\ -1.845 \\ -0.044 \end{bmatrix} \quad \mathbf{q_3} = \begin{bmatrix} 0 \\ 1.525 \\ -1.939 \\ -0.284 \end{bmatrix}$$
$$\mathbf{q_5} = \begin{bmatrix} 0 \\ 1.558 \\ -1.813 \\ -0.604 \end{bmatrix} \quad \mathbf{q_7} = \begin{bmatrix} 0 \\ 1.288 \\ -1.657 \\ -0.328 \end{bmatrix}. \tag{17}$$

By applying the optimal force distribution algorithm and solving the static problem, it results that the values of the torques required are noticeably increased due to the four-legged condition and the posture assumed (Table 7).

In the other configuration, in order to test the efficiency of the algorithm, the system is evaluated under the action of different forces and moments. The configuration chosen is the same (i.e., beginning of the step) and the force and moment vector is

$$\gamma = \begin{bmatrix} -1 \cdot 10^{-5}\ (\mathrm{N}) \\ -1 \cdot 10^{-5}\ (\mathrm{N}) \\ -F_p\ (\mathrm{N}) \\ -1 \cdot 10^{-5}\ (\mathrm{N\,m}) \\ -1 \cdot 10^{-5}\ (\mathrm{N\,m}) \\ -1 \cdot 10^{-5}\ (\mathrm{N\,m}) \end{bmatrix}, \tag{18}$$

Table 8
Distributed forces for the beginning step configuration with external forces: pseudoinverse (SX) and optimized solution (DX).

Leg	Distributed forces (μN)			Opt. distrib. forces (μN)		
	f_x	f_y	f_z	f_x	f_y	f_z
1	−2.003	−3.616	−31.752	−2.176	−3.091	−31.465
3	−1.434	−2.007	−42.017	−0.759	−2.774	−42.346
5	−2.901	−1.448	−41.692	−3.914	1.030	−41.353
7	−3.661	−2.929	−31.689	−3.150	−3.104	−31.985

Table 9
Torques related to the optimized solution for the configuration adopted at the beginning of the step.

Leg	Torques (μN m)			
	τ_1	τ_2	τ_3	τ_4
1	−3.439	−53.969	−50.130	−28.190
3	2.645	−63.860	−64.136	−33.900
5	−0.765	−57.293	−53.670	−23.955
7	−6.967	−54.125	−45.697	−23.433

where the third element is the weight. The solutions found with the pseudoinverse and the subsequent optimization, necessary because the first and eighth leg values do not satisfy the friction constraints, are shown in Tables 8 and 9.

The optimized solution for the distributed forces shows the torque values found and also shows that the friction constraint is satisfied.

4. Leg posture

In nature, the preferred spider's leg posture is the so-called C-shape configuration (i.e., hip low, knee high, ankle low; see [34]). This posture has been chosen in our model in a bio-mimetic point of view, taking into account a spider's natural behavior. Other natural systems (i.e., arthropods and insects) and artificial legged robotic systems exploit a Z-shape configuration (Fig. 5(a) and (b); see [35]).

In this section, in order to justify the chosen configuration and posture for a future robotic prototype, both an analysis and an evaluation of the efficiency of the chosen solution with respect to any other reachable configuration are made. The spider model is considered at rest on a flat horizontal surface with an approaching angle for all the legs equal to 30° ($\pi/6$ rad) and, in each case, the same configuration for all the legs ($\mathbf{q}$). The applied force considered is the weight (direction $-z$).

The effort needed for maintaining static equilibrium (E) has been defined as the sum of the absolute values of the torques that have to be applied to the 32 actuated joints:

$$E = \sum_{i=1}^{n=8} \left(\sum_{j=1}^{m=4} |\tau_{ji}| \right). \tag{19}$$

The torques are calculated by means of Eq. (13) for each angular value of the joints within the limits. The θ_4 revolute pair, with the approaching angle fixed to $\pi/6$ rad, can be avoided, because the equation

$$\theta_4 = -\frac{\pi}{6} - \theta_2 - \theta_3 \tag{20}$$

has to be always verified.

The first revolute pair θ_1 is irrelevant, because it acts on the same axis of the applied weight.

Starting from the body, the other revolute pairs are evaluated, and a sweep on their possible values is made with an iteration step of 0.1 rad. Thus, for each θ_2 value, a sweep on the possible θ_3 values that create an allowable configuration is made. By iterating from the minimum to the maximum allowable value, it is possible to compute and compare the effort. Two absolute minima can be found (see Fig. 9).

In Fig. 9, the θ_2 iteration steps are highlighted by broken lines, and for each θ_2 value a sweep on the allowable θ_3 angles is made and the overall required effort registered with an $*$.

For each θ_2 step, there is a relative minimum and a relative maximum. Concerning the θ_3 angle, the relative minimum can be found in the first half of the window of iteration (i.e., $\theta_3 < 0$) if $\theta_2 < 0$ and in the second half (i.e., $\theta_3 > 0$) if $\theta_2 > 0$. Then, in order to have a minimum, the second and third joints must be both positive or both negative. The two absolute minimum effort configurations (i.e., • in Fig. 9) are respectively for $\theta_2 = -90°$ and $\theta_2 = +90°$.

The C-shape configuration, assumed for the kinematic and static analysis of the system by taking into account the biological behavior of the real spider, does not match this condition being $\theta_2 > 0$, $\theta_3 < 0$ and $\theta_4 < 0$.

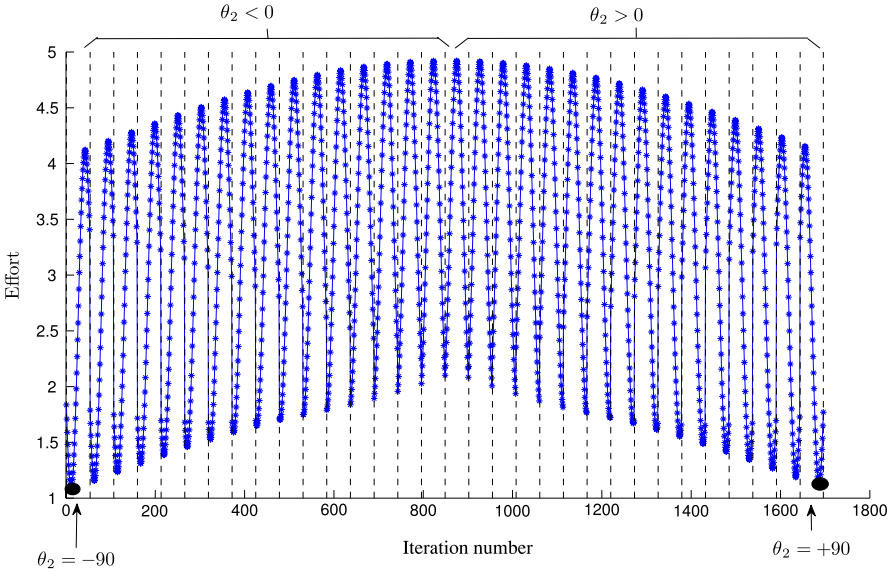

Fig. 9. Torque cost for eight support legs with an approaching angle of 30° and with respect to the number of iterations (iteration step 0.1 rad–θ_2 limits: ±90); $*$ depict the iterations on θ_3 and • the absolute minima.

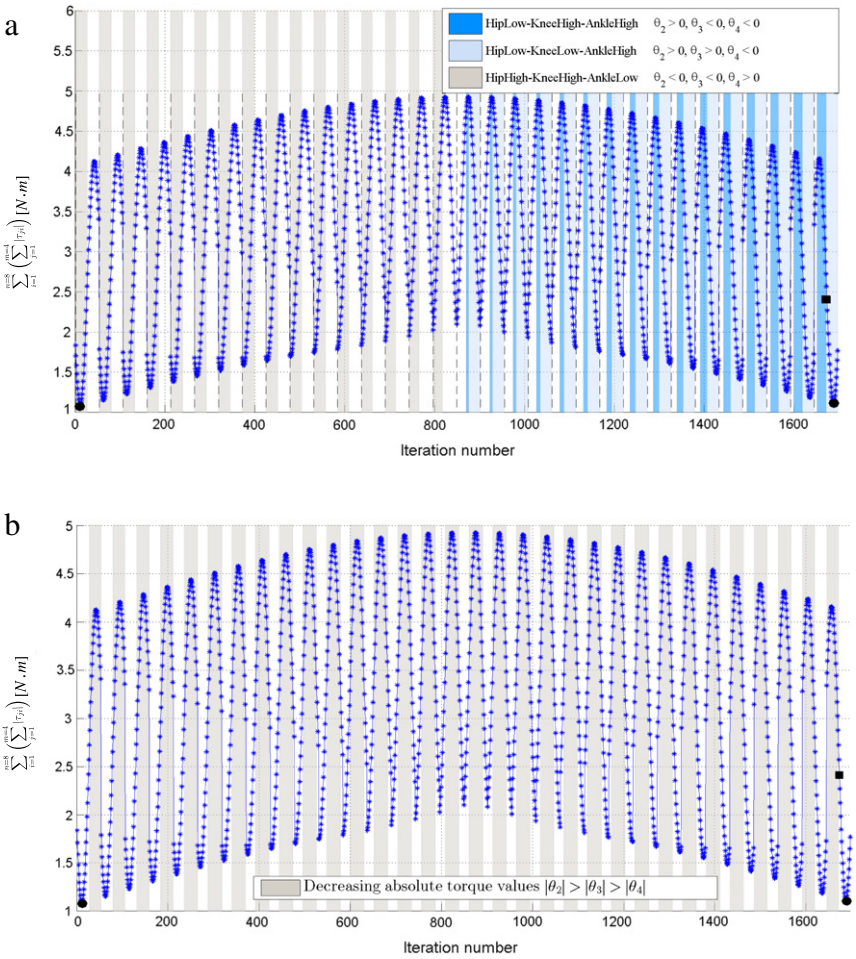

Fig. 10. Torque cost for eight support legs. Possible configurations with approaching angle of 30° and $\theta_1 = -90°$ with respect to the number of iterations. (a) The three different colors highlight the three different possible configurations; (b) gray zones represent the condition of decreasing of the required torque from the body to the last limb of the leg. (For interpretation of the references to colour in this figure legend, the reader is referred to the web version of this article.)

In order to justify the chosen configuration, a deeper analysis has to be made, and the three allowable configurations, *Hip Low–Knee High–Ankle High* with $\theta_2 > 0, \theta_3 < 0, \theta_4 < 0$ (C-shape configuration), *Hip Low–Knee Low–Ankle High* with $\theta_2 > 0, \theta_3 > 0, \theta_4 < 0$ (Z-shape configuration) and *Hip High-Knee High-Ankle Low* with $\theta_2 < 0, \theta_3 < 0, \theta_4 > 0$, have to be evaluated and compared.

In Fig. 10(a), the torque cost for all the three allowable configurations is shown using different colors.

The second and third kinds of posture allow configurations with a lower amount of torque with respect to the C-shape configuration (in Fig. 10(a) ■ is the C-shape optimum while the absolute minima are pointed out with a ●). By analyzing the torque values for each joint in the minimum effort configurations, it can be remarked that the absolute value of the torque requested to the last joint is greater than the torque requested by the other joints.

In Fig. 10(b), the zones where the condition $|\tau_2| > |\tau_3| > |\tau_4|$ holds, hence the points where the required torques decrease in a progressive manner, are depicted. From a practical point of view, this condition is of the most importance because, if satisfied, it allows motors and actuators with a decreasing power, dimension and load.

Bycomparing Fig. 10(a) and (b), it is possible to point out that the two requested conditions (i.e., C-shape configuration and decreasing torques) are satisfied in the right-hand sides of the plots. The optimum value for the C-shape configuration (pointed out with ■ in Fig. 10(a)), satisfies both the requirements.

As a conclusion, it can be said that the chosen C-shape configuration does not represent the minimum effort configuration but it is an optimum if both a low effort and a decrease of the requested joint torques from the body to the tip of the legs are considered.

5. Conclusions

In this paper, the problem of the force and torque distribution for an eight-legged bio-mimetic spider robot is addressed.

Starting from the well-known FDP, the formulation has been extended in order to control and solve the static problem not only on flat surfaces but also on vertical and inverted walls.

This has been done by considering and modeling the adhesion capabilities and limits of the spider *E. arcuata* starting from the results presented in [6,7,10,11]. Different slope conditions have been evaluated, simulated and solved.

Moreover, by considering different postures that can be found in nature (e.g., spiders and insects), an analysis of the effort required to support the overall eight-legged robotic system has been carried out, demonstrating how the C-shape spider posture allows an optimal compromise between a low effort and the requirement of a torque diminution from the body to the tip of the legs.

If a slow motion condition is considered, the static solution presented in this work can be applied in order to evaluate and solve the dynamic problem by means of a quasi-static approach.

Future work will cover on the one hand the improvement of the adhesive model, taking into account progress in bio-adhesive materials and research and, on the other hand, the construction of a working prototype.

Acknowledgements

Sincere thanks are expressed to D. Borghese and P. Perusini for their help with the implementation of the Matlab® simulators.

References

[1] A. Ijspeert, Central pattern generators for locomotion control in animals and robots: a review, Neural Networks 21 (4) (2008) 642–653.
[2] H. Cruse, D. Brunn, C. Bartling, J. Dean, M. Dreifert, T. Kindermann, Walking: a complex behavior controlled by simple networks, Adaptive Behavior 3 (1995) 385–418.
[3] G. Figliolini, P. Rea, Mechanics and simulation of six-legged walking robots, in: Climbing and Walking Robots Towards New Applications, I-Tech Education and Publishing, Austria, 2007, pp. 1–22.
[4] K. Autumn, A. Peattie, Mechanisms of adhesion in geckos, The Journal of Integrative and Comparative Biology 42 (6) (2002) 1081–1090.
[5] K. Autumn, M. Sitti, Y. Liang, A. Peattie, W. Hansen, S. Sponberg, T. Kenny, R. Fearing, J. Israelachvili, R. Full, Evidence for van der Waals adhesion in gecko setae, Proceedings of the National Academy of Sciences of the USA 99 (19) (2002) 12252–12256.
[6] A. Kesel, A. Martin, T. Seidl, Adhesion measurements on the attachment devices of the jumping spider Evarcha arcuata, Journal of Experimental Biology 206 (2003) 2733–2738.
[7] A. Kesel, A. Martin, T. Seidl, Getting a grip on spider attachment: an AFM approach to microstructure adhesion in arthropods, Smart Materials and Structures 13 (2004) 512–518.
[8] H. Gao, X. Wang, H. Yao, S. Gorb, E. Arzt, Mechanics of hierarchical adhesion structures of geckos, Mechanics of Materials 37 (2–3) (2005) 275–285.
[9] K. Autumn, Y. Liang, S. Hsieh, W. Zesch, W. Chan, T. Kenny, R. Fearing, R. Full, Adhesive force of a single gecko foot-hair, Nature 405 (2000) 681–685.
[10] A. Gasparetto, T. Seidl, R. Vidoni, Kinematic study of the spider locomotor system in a biomimetic perspective, in: Proceedings of the IEEE/RSJ International Conference on Intelligent Robots and Systems, IROS 2008, Nice, France, 2008.
[11] A. Gasparetto, T. Seidl, R. Vidoni, Passive control of attachment in legged space robots, Applied Bionics and Biomechanics 7 (1) (2009) 69–81.
[12] C. Mahfoudi, K. Djouani, S. Rechak, Optimal force distribution for the legs of an hexapod robot, in: Proceedings of 2003 International Conference on Control Applications, CCA 2003, vol. 1, 2003, pp. 657–663.
[13] X. Chen, K. Watanabe, K. Kiguchi, K. Izumi, Optimal force distribution for the legs of a quadruped robot, Journal of Machine Intelligence & Robotic Control 1 (2) (1999) 87–94.
[14] C. Klein, S. Kittivatcharapong, Optimal force distribution for the legs of a walking machine with friction cone constraints, IEEE Transactions on Robotics and Automation 6 (1) (1990) 73–85.
[15] S. Farritor, S. Dubowsky, N. Rutman, On the design of rapidly deployable field robotic systems, in: Proceedings of the 1996 ASME Design Engineering Technical Conferences and Computers in Engineering Conference, Irvine, CA, 1996.
[16] F. Cheng, D. Orin, Efficient formulation of the force distribution equations for simple closed-chain robotic mechanisms, IEEE Transactions on Systems, Man and Cybernetics 21 (1) (1991) 25–32.
[17] J. Wen, L. Witfinger, Kinematic manipulability of general constrained rigid multibody systems, IEEE Transactions on Robotics and Automation 15 (3) (1999) 558–567.
[18] Y. Yi, J. McInroy, Y. Chen, Over-constrained rigid multibody systems: differential kinematics, and fault tolerance, in: SPIE Proceedings, Smart Structures and Materials 2002: Smart Structures and Integrated Systems, San Diego, CA, 2002.
[19] D. Hong, R. Cipra, Visualization of the contact force solution space for multi-limbed robots, Journal of Mechanical Design 128 (2006) 295–302.
[20] V. Kumar, K. Waldron, Force distribution in closed kinematic chains, IEEE Journal of Robotics and Automation 4 (6) (1988) 657–664.
[21] M. Nahon, J. Angeles, Real time force optimization in parallel kinematic chains under inequality constraints, IEEE Transactions on Robotics and Automation 8 (4) (1992) 439–450.
[22] H. Liu, B. Wen, Force distribution for the legs of a quadruped walking vehicle, Journal of Robotic Systems 14 (1) (1998) 1–8.
[23] W. Chen, S.H. Yao, K.H. Low, Modular formulation for dynamics of multi-legged robots, in: Proceedings of the 7th International Conference on Advanced Robotics, Monterey, CA, 1997, pp. 279–284.
[24] J. Barreto, A. Trigo, P. Menezes, J. Dias, A.D. Almeida, FBD—the free body diagram method, kinematic and dynamic modelling of a six leg robot, in: Proceedings of AMC'98—5th International Workshop on Advanced Motion Control, 1998, pp. 423–428.
[25] J. Ayers, Building a robotic lobster, in: Artificial Ethology, Oxford University Press, Oxford, 2001, pp. 139–155.
[26] K. Safak, G. Adams, Dynamic modeling and hydrodynamics performance of biomimetic underwater robot locomotion, Autonomous Robots 13 (3) (2002) 223–240.
[27] J. Bares, D. Wettergreen, Dante II: technical description, results and lessons learned, International Journal of Robotics Research 18 (7) (1999) 621–649.
[28] M. Sitti, R. Fearing, Nanomodeling based fabrication of synthetic gecko foot-hairs, in: Proceedings of the IEEE International Conference on Nanotechnology, 2002, pp. 137–140.
[29] M. Sitti, R. Fearing, Synthetic gecko foot-hair micro/nano-structures for future wall-climbing robots, in: Proceedings of the IEEE International Conference on Robotics and Automation, ICRA'03, 2003, pp. (1)1164–1170.
[30] M. Sitti, R. Fearing, Synthetic gecko foot-hair for micro/nano structures as dry adhesives, Journal of Adhesion Science and Technology 18 (2003) 1055–1074.
[31] B. Yurdumakan, N. Raravikar, P. Ajayanb, A. Dhinojwala, Synthetic gecko foot-hairs from multiwalled carbon nanotubes, Chemical Community (2005) 3799–3801.
[32] B. Noble, Methods for computing the Moore–Penrose generalized inverse, and related matters, in: M.Z. Nashed (Ed.), Proceedings of the Advanced Seminar, The Mathematical Research Center, University of Wisconsin, New York, USA, 1976, pp. 245–301.
[33] L. Sciavicco, B. Siciliano, Modelling and Control of Robot Manipulators, Springer, London, GB, 2001.
[34] R. Foelix, Biology of Spiders, II ed., Oxford University Press, New York, USA, 1996.
[35] N. Alshurafa, J. Harmon, Artificial spider: eight-legged arachnid and autonomous learning of locomotion, in: Proceedings of SPIE-2006 the International Society for Optical Engineering, vol. 6230, p. 62301E.
[36] A. Saunders, D. Goldman, R. Full, M. Buehler, The rise climbing robot: body and leg design, Proceedings of SPIE 6230 (2006) 623017.

R. Vidoni received his M.Sc. in Electronic Engineering from the University of Udine, Italy, in 2005. In 2009, he obtained his Ph.D. degree in Industrial and Information Engineering, curriculum "Applied Mechanics" from the University of Udine, Italy. His research interests include bio-robotics, trajectory planning and modeling and control of flexible-link mechanisms.

A. Gasparetto obtained his M.Sc. degree in Electronic Engineering from the University of Padova, Italy, in 1992. In 1996, he obtained his Ph.D. in Applied Mechanics from the University of Brescia, Italy. In 2003, he obtained his M.Sc. degree in Mathematics from the University of Padova, Italy. Currently he is a Full Professor of Mechatronics and Mechanics of Robots at the Faculty of Engineering of the University of Udine. The research activity of Prof. Gasparetto is in the fields of mechatronics, robotics and vibration mechanics.